Shape control of CdSe/CdS nanocrystals during shell formation and growth: Dominating effects of surface ligands over core crystal structure

Junjie Hao, Haochen Liu, Xijian Duan, Ziming Zhou, Bingxin Zhao, Wenda Zhang, Bing Xu, Xiao Wei Sun, Marie-Hélène Delville

mater.scichina.com link.springer.com

Shape Control of CdSe/CdS Nanocrystals During Shell Formation and Growth: Dominating Effects of Surface Ligands Over Core Crystal Structure

Junjie Hao[1,2,3#*], Haochen Liu[2,4#], Xijian Duan[2,5], Ziming Zhou[2,5], Bingxin Zhao[2], Wenda Zhang[2,7], Bing Xu[6], Xiao Wei Sun[2,5,6*], Marie-Helene Delville[1*]

ABSTRACT **CdSe/CdS nanocrystals (NCs) are among the most studied, yet, there is still much information to be gained. This work reveals that core@shell NCs with different shapes are more controlled by the interaction between the NC surface and the capping ligands than the core concentration, and not at all by the difference in the crystalline nature of the core. Among the precursors, cadmium carboxylates promote an isotropic structure while conversely, long-chain cadmium phosphonates favor an anisotropic one. Cadmium carboxylates are critical in the formation of the headshell while cadmium phosphonates play a role in the anisotropic tail growth. Against expectations, the CdSe-core crystal structure (zinc blende or wurtzite) plays very little role in determining the structure of the final shape, which may be due to the two-stage CdS shell formation process, and gives rise to a tadpole shape. With appropriate capping ligands, precise control of the CdSe/CdS structures can be achieved in both shape formation and growth process. We claim, here, that CdSe/CdS with morphologies as different as tadpoles, nanoflowers, dot-in-rods, and tetrapods are obtained with only varying surface ligand ratios. This unique crystal-growth mechanism can be applied to other seed-mediated methods to produce anisotropic nanostructures.**

Keywords: Tadpole shape, CdSe/CdS NCs, Shell growth control, Effects of surface ligands, Core crystal structure

INTRODUCTION

The synthesis of core@shell colloidal semiconductor NCs with controlled size and shape in their quantum confinement size regime has been very successful in the last two decades [1-7]. Extensive studies have revealed that they are of great interest for catalysis [8, 9], optoelectronics [10, 11], chirality [12, 13], and self-assembly. The most interesting NCs should not only be highly monodispersed in size but also have a unique shape. Unfortunately, even for the most studied CdSe/CdS NC systems, the structural perfection of the NC form has not yet reached a satisfactory level, especially from the point of view of anisotropy. The results described below suggest that, instead of considering the crystal structure of the core, it is also mandatory to take into account the crystal interface and the effects of surface ligands as well as the core concentration to control the shape uniqueness. In the specific case of the CdSe/CdS NCs with a tadpole shape, we will show that surface effects dominate and control the differences in shape during both the formation and the growth of the CdS shell.

Recently, the seed-mediated core@shell growth method was tried to produce anisotropic NCs. Compared to the one-pot synthesis, it improves the nucleation-growth processes, with better control of the mono-dispersity and the uniformity of the morphology [1, 6, 14-16]. Anisotropic NCs exhibit optoelectronic properties different from those

[1] CNRS, Univ. Bordeaux, Bordeaux INP, ICMCB, UMR 5026, Pessac, F-33608, France
[2] Institute of Nanoscience and Applications and Department of Electrical and Electronic Engineering, Southern University of Science and Technology, Shenzhen, 518055, China
[3] College of Integrated Circuits and Optoelectronic Chips, Shenzhen Technology University, Shenzhen, 518118, China
[4] Department of Materials Science and Engineering, and Centre for Functional Photonics (CFP), City University of Hong Kong, Hong Kong SAR, 999077, P.R. China
[5] Key Laboratory of Energy Conversion and Storage Technologies (Southern University of Science and Technology), Ministry of Education, Shenzhen, 518055, China
[6] Shenzhen Planck Innovation Technologies Co. Ltd., Shenzhen, 518173, China
[7] Hainan Provincial Key Laboratory of Fine Chemicals, Hainan University, Haikou, 570228, China
[#] *These authors contributed equally to this work*
[*] Corresponding author (email: marie-helene.delville@icmcb.cnrs.fr; sunxw@sustech.edu.cn; haojunjie@sztu.edu.cn)

of the spherical quantum dots (QDs) due to dimension-dependent quantum confinement [2, 17-21]. In particular, anisotropic core@shell NCs have both efficient charge separation and efficient carrier transport, which make them promising in a wide range of optoelectronic applications, for instance, photovoltaics [22], electron transistor [23], optical strain gauge [24], chirality [12, 13, 25], and photocatalysis [8, 9]. The anisotropic morphology of shells mainly arises from a dissimilar growth rate in different spatial directions due to a difference in surface energy between the different crystal facets of the cores [6]. The usual strategy to induce a break in shell symmetry growth is to use extra ligands such as phosphonic acids [2, 18] and halides [26]. They selectively bind onto specific facets of the crystals controlling their surface energy and their growth rate. The side facets of the wurtzite (W) rods and tetrapods are typically nonpolar ones and claimed to be stabilized by the so-called "cadmium-phosphonic acid complexes" [27, 28]. Generally speaking, the preparation of polar NCs with specific shapes often requires an alternation of isotropic and anisotropic growth processes. This means that a secondary shell growth process is always needed [6, 15, 16], complicating the overall preparation and increasing its cost because of repeated purifications and re-growth stages.

In this work, we propose an alternative way with a two-type ligand-mediated core@shell growth method based on a controlled combination of mixed cadmium-phosphonic acid and cadmium-carboxylic acid complexes acting as ligands. This method then differs from the most commonly used single-type ligand syntheses, in that it controls both the morphologies and sizes of the NCs [1-4, 24]. No additional purification or injection processes are required, and the anisotropic growth is achieved in a *single* one-pot process. This method assumes that the shape control of the CdSe/CdS NCs is regulated by the strength of the bond interaction of these ligands with the exposed surface ions of the NCs. Based on previous results [29, 30], a more systematic study of the different capping ligands and, more specifically, their ratios, was performed here to control and understand the formation of specific shapes other than the known rods or tetrapods.

EXPERIMENTAL SECTION

Synthesis of CdSe/CdS Tadpoles

In a typical synthesis of CdSe/CdS Tadpoles *via* the seeded growth procedure, the seeding solution consisted of CdO (115.8 mg, 0.9 mmol) mixed, in a 50 mL flask, with tri-n-octyl phosphine oxide (TOPO, 3 g, 7.76 mmol), n-octadecyl phosphonic acid (ODPA, 285 mg, 0.852 mmol) and oleic acid (OA, 908 mg, 1.02 mL, 3.21 mmol). The resulting mixture was heated first at 150 °C and purged with five vacuum/argon cycles, then at 320 °C to obtain a completely transparent solution, and dissolve all the solids. Because of the mixture of ODPA and OA ligands, the reaction rate was very slow and took more than 2 hours, as opposed to pure ODPA or OA systems; for instance, only 30 minutes are required in the case of pure ODPA with a transparent light-yellow solution instead of colorless. After 1.5 mL of tri-n-octyl phosphine (TOP) were added and the temperature maintained at 320 °C, 50 nmoles of the previously obtained W-CdSe-TOP solution were introduced. The S-TOP (0.5 M, 3 mL, 1.5 mmol) was divided into four incremental injections at 2-minute intervals (0, 2, 4, and 6 minutes). The CdSe/CdS NCs were allowed to grow at 320 °C, for approximately 8 minutes after the W-CdSe core injection. Aliquots were removed from the reaction mixture at different time intervals and diluted in chloroform. Finally, the reaction mixture was cooled down to room temperature and an extraction procedure was used to separate the NCs from the side products and unreacted precursors. For control experiments, the S-TOP was also injected in one shot.

Synthesis of Different Shapes of CdSe/CdS NCs Based on W-CdSe

Nanoflowers, three-tail, and two-tail Tadpoles, DRs, and tetrapods were synthesized by a process identical to that for the one-tail Tadpole NCs. We just worked on the chemical nature of the ligands, their ratios, and/or the core concentration. For instance, a nanoflower shape can be obtained using ODPA (0 mg, 0 mmol) and OA (1.02 mL, 3.21 mmol); a three-tail Tadpole requires ODPA (100 mg, 0.299 mmol) and OA (1.02 mL, 3.21 mmol), while a two-tail Tadpole needs ODPA (150 mg, 0.448 mmol) and OA (1.02 mL, 3.21 mmol). Different aspect ratios (AR) for DRs can also be obtained by changing the ligand ratios: for example, ODPA (633 mg, 1.89 mmol) and HPA (0 mg, 0 mmol), or ODPA (600 mg, 1.79 mmol) and HPA (162 mg, 0.975 mmol). The Tetrapod shape can be synthesized by the same process as for DRs, just decreasing the amount of CdSe cores from 50 nmoles to 5 nmoles.

RESULTS AND DISCUSSION

By designing the reaction system as illustrated below, it is possible to separate the initial nucleation stage from the subsequent growth process, and somewhat demonstrate different trends in the ligand effects. W-CdSe cores with a 2.8 nm diameter were used as starting materials. All the experiments were performed at 320 °C in the presence of various ratios of ODPA and OA as capping agents. Other parameters such as the variation of the core concentration, the

incremental injection, and the one-shot of the solution sulfur were also carried out and mentioned when necessary.

The effects of ODPA as a source of symmetry breaking

We first performed the experiments by adding sulfur in four incremental-solution injections (see the experimental section for more information). Since ODPA is known as a key factor for the anisotropic growth of W-CdSe/W-CdS NCs [15, 17, 21, 24, 27, 31], we undertook a systematic study of its influence as an OA-disrupting ligand by varying its ratio up to 20%. The main morphologies and their ultraviolet-visible (UV-vis.) and photoluminescence (PL) spectra are presented in Fig. 1 and Fig. S1-S2. They significantly illustrate the role played by this phosphonic acid. In the absence of such a ligand (large excess of OA), the obtained nanoflower-like morphology can be considered symmetric (Fig. 1a) compared to those obtained (Fig. 1b-d) after the addition of ODPA, even in a small amount.

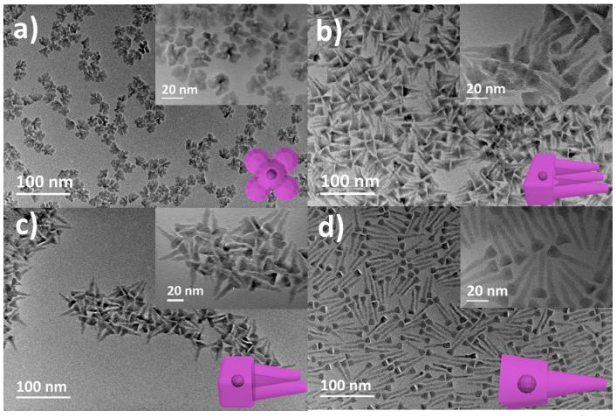

Figure 1 Transmission electron microscope (TEM) images of the evolution of the different shapes of W-CdSe/W-CdS NCs when changing the molar ratio ODPA/(ODPA+OA), for a constant amount of OA of 1.02 mL (3.21 mmol). (a) ODPA, 0%; (b) ODPA, 100 mg, 8.5%; (c) ODPA, 150 mg, 12.3%; (d) ODPA, 285 mg, 20.9%.

These experiments confirm the suggestions made by Alivisatos *et al.* [15] and Cheon *et al.* [1] who claimed that the surface energy of the NCs is modulated by introducing surfactants that are susceptible to adsorb onto the different surfaces of the growing crystallites. The difference in the growth rate between the different crystallographic directions is, thus, accentuated [1, 15]. Then, because of the much stronger binding between the cadmium cation and the phosphonate anion [32, 33], the presence of additional ODPA in the cadmium precursor solution drastically changes the composition of the ligands around the CdSe core; this, in turn, modifies the shape of the growing NC. Indeed, for a given amount of OA when no additional ODPA is introduced the resulting nanoobjects exhibit a rather symmetric growth with a resulting nanoflower morphology (Fig. 1 a, Table S1). This is probably because the amount of ODPA released into the solution from that preexisting on the core surface is too small to induce any symmetry breaking during the growth process.

However, when adding and adjusting the amount of ODPA in the injection solution and therefore adjusting the ligand ratios (ODPA/(OA+ODPA) = 8.5, 12.3, 20.9%), other morphologies were obtained and named Tadpoles henceforth (Fig. 1 b-d, Table S1). With the increase in anisotropy, the diameter gradually decreases and the quantum yield gradually increases (Table S2). The head of the Tadpoles, their aspect ratio (AR), and the number of tails systematically decrease when the ODPA ratio increases confirming, here in a nice way, the strong implication of ODPA not only in symmetry breaking but also in morphology anisotropy. It also confirmed its selective binding to the {100} and {110} surfaces of the growing crystallites, orientating the growth pattern along the [001] direction to eventually form a long tail. In the absence of ODPA or at low concentrations, due to the weak "selective adhesion" process, the faceted NCs form flowers and Tadpoles with three and two tails. When an increased ratio of the ligand with "selective adhesion" (ODPA), the Tadpole shape with a single tail prevails. The presence of these surface ligands was confirmed by NMR (Fig. S3) where besides the peaks in ^{31}P NMR spectrum of free TOPO is at δ = 48.7 ppm and that of free at δ = 30 ppm we observe the large ^{31}P NMR peak of coordinated ODPA centered at 25ppm in good agreement with the variety of possible binding modes of the phosphonate to the NCs surface, which shift to lower fields with respect to the free phosphonic acid. In fact, in between ($Cd(OA)_2$) and ($Cd(ODPA)_2$), cadmium dicarboxylate is the most reactive and participates first to generate a symmetric shell around the CdSe core.

Characterization of Tadpole shape NCs based on W-CdSe

The experimental conditions found to obtain Tadpoles as in Fig. 1d are reproducible as shown in Fig. 2 (50 nmol CdSe Cores, ODPA (285 mg, 0.85 mmol), and OA (1.02 mL, 908 mg, 3.21 mmol)), and are referred to as Reference Conditions (RC). This Figure also provides the physical-chemical characterizations of this type of morphology. Fig. 2a shows a representative high-magnification transmission electron microscope (TEM) image of these CdSe/CdS Tadpoles.

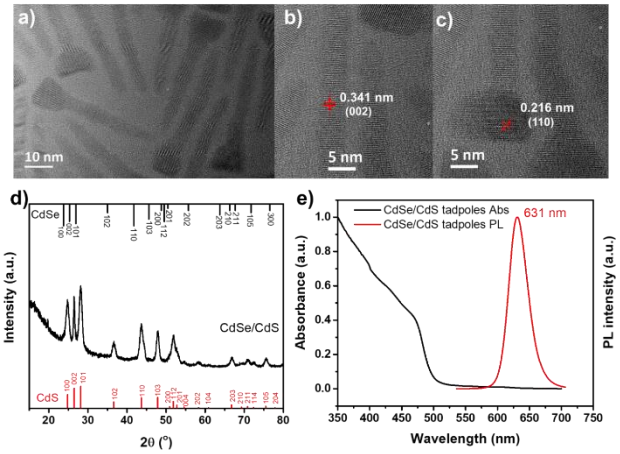

Figure 2 (a) Representative TEM image of CdSe/CdS Tadpoles; (b) High-resolution TEM (HR-TEM) images of the tail of a Tadpole NC; (c) HR-TEM images of the head of a Tadpole NC; (d) X-ray diffraction (XRD) pattern of CdSe/CdS Tadpoles; (e) UV-vis. and PL spectra of CdSe/CdS Tadpoles.

They exhibit a head bigger (see Fig. S4 for the definition of the head and tail) than the core precursor, prolonged by a single long tail: see also a large area image in Fig. S5 This morphology is very different from the already reported dot-in-rods (DRs) or tetrapods obtained with conventional seeded growth procedures [2, 17, 24, 26, 27]. As shown on the high-resolution TEM (HR-TEM) image of a single Tadpole (Fig. 2b), the lattice fringes of the tail have an interplanar spacing of 0.341 nm, corresponding to (002) planes of the CdS wurtzite phase.

The lattice fringes of the head in Fig. 2c show a clear hexagonal packing pattern with the 0.216 nm d-spacing corresponding to (110) crystal planes of the W-CdS. This indicates that the Tadpole does grow along the c-axis of the W phase. The CdS shell crystallizes in the wurtzite type for the whole core@shell NCs, in agreement with the literature, which mentions that CdS prefers to grow in the wurtzite phase starting from W-CdSe seeds [2]. These data are confirmed by the X-ray diffraction (XRD) pattern in Fig. 2d, which also shows a wurtzite crystal structure for the CdSe/CdS Tadpoles (CdSe: *JCPDS* 08-0459 and CdS: *JCPDS* 41-1049). The intense and sharp peak of the (002) crystal planes suggests that a long (002) domain of the wurtzite phase is present in the Tadpole [26, 27, 34] and consistent with the HR-TEM data in Fig. 2b. The optical properties of the Tadpoles are typical: a broad band of the CdS absorption below 500 nm in UV-vis. absorption spectroscopy and a peak at 631 nm in PL spectroscopy (Fig. 2e). A more specific study shows the variation in the NC absorption and PL spectra all along the reaction process (Fig. S6). TEM analysis confirmed these modifications in sizes and shapes (Fig. 3, Table S3). The first excitonic absorption peak shifts downward with time (from 0 to 8 minutes) (Fig. S6a), as typically observed during CdS shell growth [3, 35]. As the CdS goes on depositing on NCs (Fig. 3), the intensity of the broad absorption band below 500 nm gradually increases (Fig. S6a).

Additionally, the PL maximum wavelength redshifts from 554 to 631 nm with, first, a decrease and then an increase of the full width at half maximum (FWHM) (Fig. S6b). Such significant red shifts can be regarded as a signature of successful epitaxial growth of the shell, instead of serious alloying between the core and shell [3, 36]. This FWHM decrease is attributed to the reduction in the particle size distribution during the epitaxial growth; the subsequent band broadening likely results from the directional growth of the objects and the inhomogeneity of the final Tadpole structures.

TEM analyses were performed on at least 200 nanoobjects obtained after reactions run over different times (Fig. 3) to investigate the growth mechanism, especially the tail growth process starting from W-CdSe seeds. As shown in the line scanning images (Fig. S7), the CdSe core is located at the head of the Tadpole NCs. They show that the Tadpole growth process seems to be divided into two main stages (Scheme 1, the two-stage growth process of the four morphologies are present in Scheme S1). Stage 1 is the formation of a wurtzite-type CdS shell around the core (Fig. 3 b-c) [1, 2]; it easily forms at such a high reaction temperature (320 °C) since, at this temperature, CdS adopts a wurtzite crystal phase whether the seeds are of the W- or zinc blende (ZB-) type [1, 2]. This initial spherical shape of W-CdSe/CdS (< 2 minutes) is due to the high reactivity of cadmium dicarboxylate [35], which first coordinates to the CdSe surface and forms an isotropic CdS layer leading to an isotropic growth. It is followed by a so-called stage 2, with the preferential coordination on the {100} and {110} surfaces of phosphonate ligands that reduce the growth of these faces and favor the tail growth along the [001] direction to achieve this specific morphology (Scheme 1 and Fig. 3 d-f). This was also confirmed by control experiments using OA first followed by the subsequent ODPA addition (Fig. S8), the tail of the NCs gradually grew after the addition of ODPA (Fig. S8 c and d).

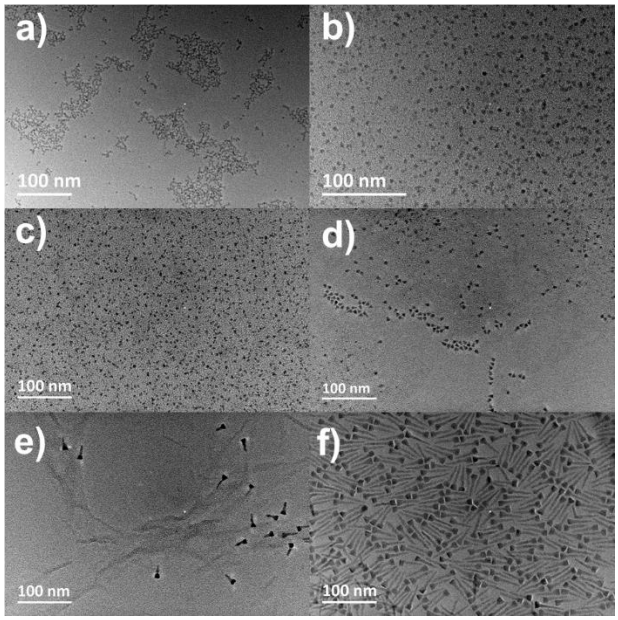

Figure 3 TEM images showing the size variation of CdSe/CdS Tadpoles with time during their synthesis starting from W-CdSe and 1.02 mL OA and 20.9% ODPA: (a) CdSe core (S0); (b) 0.5 min (S2); (c) 1 min (S3); (d) 2 min (S4); (e) 4 min (S5); (f) 8 min (S1, RC).

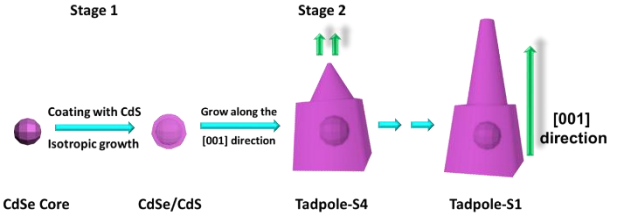

Scheme 1 A two-stage growth process of the Tadpole morphology with, in the first stage, the isotropic CdS shell growth; then in stage 2, the Tadpole shape gradually forms by shell growth along the *c* direction.

This hypothesis is also illustrated by literature data, which show that cadmium diphosphonates foster the growth of tetrapods and anisotropic rods [27, 28, 37], as opposed to cadmium dicarboxylates which favor the growth of isotropic QDs [3, 35, 36, 38]. This difference between carboxylate and phosphonate ligands in inducing such different shapes links directly to their respective coordination ability. Indeed, a phosphonate group can coordinate with up to three or more cation centers, instead of one (or two) for the carboxylate group, the phosphonate is also bigger and then less polarized than the carboxylate [35, 39, 40]. This is why the use of a mixture of these two ligands to complex Cd^{2+} cations in the precursor solution, yields W-CdSe/CdS with a Tadpole shape and very high structure purity (~ 100% in Fig. S5). The study of these ligand ratios shows that introducing ODPA not only increases the tail length but also decreases the head size (Table S1), blocking the access of OA to the surface even if it is still in excess. This was also confirmed by the control experiments using ODPA first and then adding OA (Fig. S9).

The effects of OA: from DRs to Tadpoles

To study the impact of OA on Tadpole growth, we first varied its concentration at a fixed ODPA content (285 mg, 0.85 mmol), as shown in Fig. 4 (a-e) and Table S4.

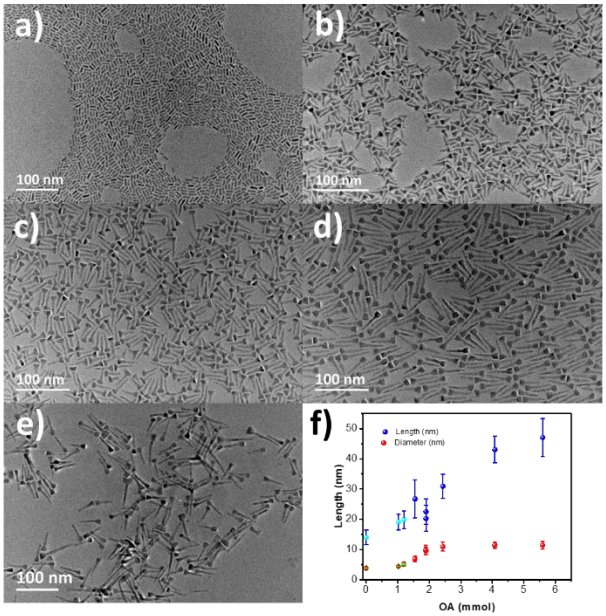

Figure 4 TEM evolution of the different shapes with the ratio of OA ligand, ODPA being constant (285 mg, 0.85 mmol). (a) OA volume (mL), (molar % (OA/(OA + ODPA))), 0 mL (0); (b) OA, 0.33 mL (55.0); (c) OA, 0.5 mL (65.0); (d) OA, 1.02 mL (79.1); (e) OA, 1.5 mL (84.8); (f) variation of the length with the OA molar content.

We also investigated the formation process of the tadpole head, choosing a total molar amount of ligands (OA + ODPA = 1.89 mmol) and varying their ratio to cover a range (OA/(OA + ODPA)) from 0 to 85% (Table S4). In the absence of OA, nanorods are formed (Fig. 4(a)). The addition of OA not only induces an asymmetric growth of the nanoobject (Fig. 4(b-e)) but also influences the length of the nanostructure formed. Indeed, the size of the Tadpole head tends to rapidly reach a limit value of 11 nm with the increase in OA ratio (Fig. 4(f)), while the tail length goes on increasing. Assuming no dissolution of the CdSe cores takes place, we explain this result with an increase in the reaction rate, which seems to be linearly dependent on the acid concentration.

At a constant concentration of ODPA, increasing the OA content in the system changes the composition of the

cadmium complexes ratio. This also induces a modification of this composition at the available surface areas of the NC head and increases its size. This CdS shell thickness increase is also characterized by the redshift of the first exciton absorption peak (Fig. S10). This is, once again, consistent with the two stages described above: (1) the first stage growth and the high activity of cadmium carboxylate complexes, and (2) the subsequent growth of CdS along the [001] direction to form the long tail.

However, the homogeneity in the Tadpole morphology can decrease, and some tetrapods appear when the OA ratio is too high (OA, 1.5 mL). In addition, the anisotropic growth of the CdS tail decreases with the decreasing OA ratio. We, therefore, chose the 1-mL OA sample as the best one to further study the effects of ODPA.

All these combined results confirm that the effects of the ligands on the tail and the head growth stages are separated. In fact, by playing on the difference in (i) reactivity between $(Cd(OA)_2)$ and $(Cd(ODPA)_2)$ on the one hand and (ii) the respective binding strengths of the Cd-bound ligands, on the other hand, it becomes possible to fine-tune and target the desired CdSe/CdS morphology.

The influence of the concentration of the CdSe cores on Tadpole shape

Experiments performed to grow Tadpoles with high ARs revealed that both length and selectivity in the Tadpole shape also depended on the concentration of the cores in the solution. To investigate this role, a series of shell growth experiments using various concentrations of W-CdSe cores were undertaken. With the ligand ratio of the reference condition (RC), (Fig. 5), we observed several phenomena as soon as we decreased the concentration of the cores: (i) the tadpole shape was maintained, (ii) the tadpole tail significantly increased, and (iii) the same applied to the aspect ratio, with tadpoles reaching a total length of 181 nm (Fig. 6) and an AR of nearly 9 (Table S5). As shown in Fig. S11, all the samples exhibit a large Stokes shift in UV-vis. spectra.

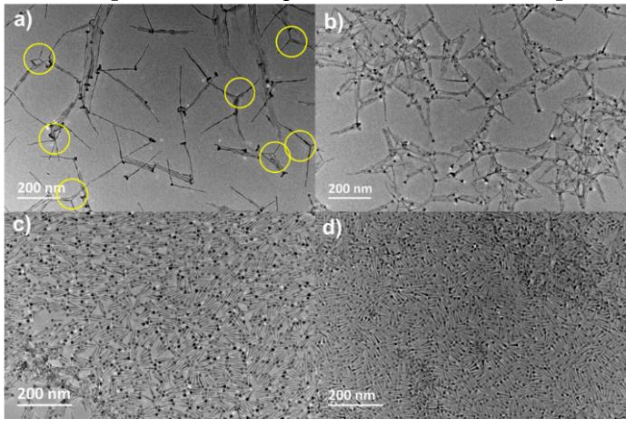

Figure 5 Effect of the concentration of the cores on the morphology of the resulting nanoobjects. (a-d). The ligands are OA (1.02 mL, 3.21 mmol), and ODPA (285 mg, 0.85 mmol), and the cores concentrations are (a) 5 nmol, (b) 15 nmol, (c) 50 nmol (RC), and (d) 100 nmol, respectively.

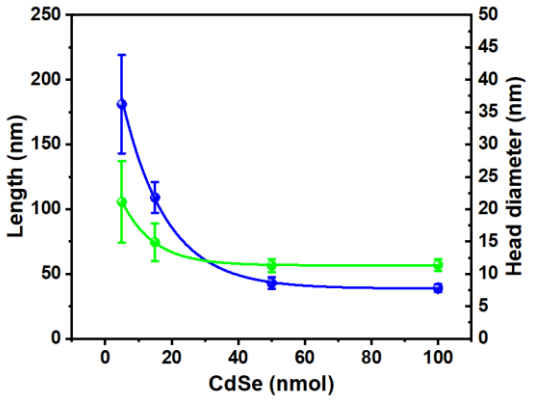

Figure 6 Variation of the Tadpole length (blue) and head diameter (green) with the concentration in seeds. Lines are guides for the eyes.

On the contrary, the tail diameter (measured systematically at the beginning of the tail position) remains unchanged (5.5-6 nm). This constancy in the diameter is due to an identical ratio between the two ligands (ODPA and OA) adsorbed on the tail surface, at this time of the reaction, in all the experiments.

However, for a low concentration of the cores (5 nmol), the final structural purity of the NCs becomes gradually poorer (Fig. 5 a-b) with the formation of tetrapods (yellow circles in Fig. 5 a). Indeed, in such a case, the relative concentrations of Cd^{2+} and S^{2-} are so high, that the CdS growth around each core becomes isotropic, and a tetrapod forms as previously reported [2, 15, 21, 24, 27, 31]. This phenomenon also appears in the case of DR synthesis. This process uses typical cadmium phosphonates for a 1D shape control, as shown in Fig. S12 (ODPA and HPA at two different concentrations) where a tetrapod shape forms at low core concentrations (5 nmol), while a DR shape is obtained at a concentration ten times higher (50 nmol).

We also used ZB-CdSe QDs as seeds to check whether the crystal structure of the core was a key parameter or not. Tadpole-shaped NCs were obtained regardless of the crystal structure of the core as illustrated in Fig. S13, which represents Tadpoles obtained by reacting 15 nmol of ZB-CdSe seeds with ODPA (285 mg, 0.85 mmol, 20.9%) and OA (1.02 mL, 908 mg, 3.21 mmol) (Table S6).

All these results (Fig. 5b, Fig. S13, and Table S6) reveal that the use of a mixture of cadmium diphosphonate and

dicarboxylate complexes under identical reaction conditions promotes the growth of a Tadpole shape no matter the crystal structure of the initial cores [35]. This is consistent (i) with the fact that the core composition at this temperature is not a key parameter, and (ii) with our hypothesis that the morphology of the Tadpole CdSe/CdS NCs during both the shell formation and the growth stage is determined mostly by the interface and the chemical nature of the ligands present at this interface. This confirms the above-mentioned two-stage mechanism, with the first growth of the Tadpole head followed by that of the tail.

In this approach, we underlined that playing with mixed ligands controls the difference in growth rates between the different crystallographic directions in the first stage. Regardless of the seed crystal structure, the addition of cadmium dicarboxylate complexes promotes the growth of NCs heads and provides Tadpole morphologies that are difficult to obtain with a single ligand. The final size of the head is bigger in the case of ZB-CdSe cores (3.95 nm) than W-CdSe, with a CdS shell thicker in the first stage, maybe because this structure exposes faces that have a different packing density on the surface of the initially formed NC. At the considered temperatures, rates of ligand adsorption and desorption on the surface of the ZB NCs being faster than that of the W NCs can also be an explanation [7].

We checked the temperature, often a crucial parameter in such a synthesis, and tested two lower ones, 260 °C and 290 °C (Fig. 7) (50 nmol of W-CdSe cores with ODPA (285 mg, 0.85 mmol, 21.2%) and OA (1.02 mL, 908 mg, 3.21 mmol)) (Table S7). At 260 °C, only distorted tetrahedral nanoparticles, with AR = 1.5, formed, meaning that a very short tail was grown at this temperature. Furthermore, the lattice fringes at d = 0.351 nm correspond to the (002) planes of the W-CdSe phase, confirming that only a thin CdS shell formed. In contrast, at 290 °C, a 19 nm tail Tadpole formed effectively. The interplanar lattice spacing of d = 0.341 nm corresponds to the (002) planes of the W-CdS phase (see the HR-TEM images of a single Tadpole, Fig. 7 b,d).

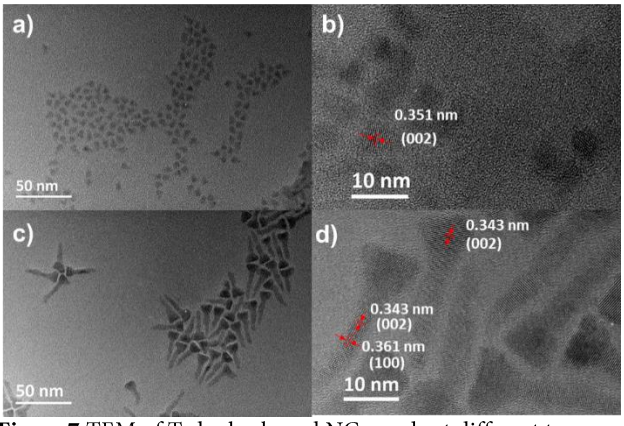

Figure 7 TEM of Tadpole-shaped NCs made at different temperatures. (a) 260 °C, (c) 290 °C; (b) and (d) are the corresponding HR-TEM images.

Therefore, this synthesis is both ligand-ratio- and temperature-dependent; it provides a broader set of solutions to control the size and shape of these Tadpoles and their subsequent properties.

One-shot injection of the shell precursors

We eventually investigated the impact of the injection mode on the resulting nanoobjects comparing the four incremental injections used above to a single shot keeping all the other parameters identical, as for the synthesis of Tadpoles in Fig. 1 d and Fig. S5. The resulting Tadpoles had the same size, but the one-shot injection was less selective and gave rise to a higher number of tetrapods (Fig. S14). We also confirmed that in the presence of a high concentration of precursors, the uniformity of the objects' morphology was destroyed (results not shown).

CONCLUSIONS

By adjusting the ratio between two functional ligands usually used separately in the synthesis of CdSe/CdS NCs, (OA and ODPA), we performed a one-pot synthesis of nanostructures with different controlled morphologies such as Tadpoles, nanoflowers, DRs, and tetrapods. In contrast to previous works [2, 24], this study shows that the one-pot synthesis of anisotropic CdSe/CdS with a Tadpole shape, in the commonly known size range, *i.e.*, 22 to 180 nm, is possible with well-chosen ligands, this regardless of the initial crystal structure (W- or ZB-) of the CdSe seeds. The CdSe core concentration and the ratio between the two chosen ligands have more influence than the crystal structure of the core on the anisotropic CdS shell growth, and in determining the shape of CdSe/CdS NCs, *i.e.*, Tadpoles versus nanoflowers, DRs, and tetrapods.

These astutely mixed ligands promote the formation

of these various shapes playing on both nucleation and growth. Cadmium oleate improves early isotropic growth, and cadmium phosphonate determines the anisotropy structure. The influence of the temperature is negligible, as is that of the core concentration and crystal structure. This controllable polytypism provides new insights into symmetry breaking and morphology anisotropy formation in colloidal NCs synthesis. This kinetically controlled strategy can be potentially extended to other NC syntheses, providing an alternative protocol for morphology control. We anticipate various anisotropic shapes, which can be useful in designing chirality probes, anisotropic catalysts, and complex optoelectronic transistors with semiconductor NCs.

Received xx-xx 2015; accepted xx-xx 2015;
Published online xx-xx 2015

1 Jun Y-w, Choi J-s, Cheon J. Shape control of semiconductor and metal oxide nanocrystals through nonhydrolytic colloidal routes. Angew Chem Int Ed, 2006, 45: 3414-3439
2 Talapin DV, Nelson JH, Shevchenko EV, et al. Seeded growth of highly luminescent CdSe/CdS nanoheterostructures with rod and tetrapod morphologies. Nano Lett, 2007, 7: 2951-2959
3 Li JJ, Wang YA, Guo W, et al. Large-scale synthesis of nearly monodisperse CdSe/CdS core/shell nanocrystals using air-stable reagents *via* successive ion layer adsorption and reaction. J Am Chem Soc, 2003, 125: 12567-12575
4 Chen O, Zhao J, Chauhan VP, et al. Compact high-quality CdSe–CdS core–shell nanocrystals with narrow emission linewidths and suppressed blinking. Nat Chem, 2013, 12: 445-451
5 Menagen G, Macdonald JE, Shemesh Y, et al. Au growth on semiconductor nanorods: Photoinduced versus thermal growth mechanisms. J Am Chem Soc, 2009, 131: 17406-17411
6 Wang X, Chen S, Thota S, et al. Anisotropic arm growth in unconventional semiconductor CdSe/CdS nanotetrapod synthesis using core/shell CdSe/CdS as seeds. J Phys Chem C, 2019, 123: 19238-19245
7 Xie R, Zhou M. Zinc chalcogenide seed-mediated synthesis of CdSe nanocrystals: Nails, chesses and tetrahedrons. Chem Mater, 2015, 27: 3055-3064
8 Nakibli Y, Kalisman P, Amirav L. Less is more: The case of metal cocatalysts. J Phys Chem Lett, 2015, 6: 2265-2268
9 Chen Y, Zhao S, Wang X, et al. Synergetic integration of $Cu_{1.94}S$–$Zn_xCd_{1-x}S$ heteronanorods for enhanced visible-light-driven photocatalytic hydrogen production. J Am Chem Soc, 2016, 138: 4286-4289
10 Yang L, Zhou Z, Song J, et al. Anisotropic nanomaterials for shape-dependent physicochemical and biomedical applications. Chem Soc Rev, 2019, 48: 5140-5176
11 Castelli A, Dhanabalan B, Polovitsyn A, et al. Core/shell CdSe/CdS bone-shaped nanocrystals with a thick and anisotropic shell as optical emitters. Adv Opt Mater, 2020, 8: 1901463
12 Xiao L, An T, Wang L, et al. Novel properties and applications of chiral inorganic nanostructures. Nano Today, 2020, 30: 100824
13 Agrawal B, Maity P. Recent developments for the synthesis of air stable quantum dots. Rev Adv Mater Sci, 2017, 49: 189-205
14 Reiss P, Protière M, Li L. Core/shell semiconductor nanocrystals. Small, 2009, 5: 154-168
15 Manna L, Scher EC, Alivisatos AP. Synthesis of soluble and processable rod-, arrow-, teardrop-, and tetrapod-shaped CdSe nanocrystals. J Am Chem Soc, 2000, 122: 12700-12706
16 Milliron DJ, Hughes SM, Cui Y, et al. Colloidal nanocrystal heterostructures with linear and branched topology. Nature, 2004, 430: 190-195
17 Sitt A, Salant A, Menagen G, et al. Highly emissive nano rod-in-rod heterostructures with strong linear polarization. Nano Lett, 2011, 11: 2054-2060
18 Fiore A, Mastria R, Lupo MG, et al. Tetrapod-shaped colloidal nanocrystals of II−VI semiconductors prepared by seeded growth. J Am Chem Soc, 2009, 131: 2274-2282
19 Zheng W, Wang Z, van Tol J, et al. Alloy formation at the tetrapod core/arm interface. Nano Lett, 2012, 12: 3132-3137
20 Rowland CE, Fedin I, Zhang H, et al. Picosecond energy transfer and multiexciton transfer outpaces auger recombination in binary cdse nanoplatelet solids. Nat Mater, 2015, 14: 484
21 Wu K, Hill LJ, Chen J, et al. Universal length dependence of rod-to-seed exciton localization efficiency in type i and quasi-type ii CdSe@CdS nanorods. ACS Nano, 2015, 9: 4591-4599
22 Tong SW, Mishra N, Su CL, et al. High-performance hybrid solar cell made from CdSe/CdTe nanocrystals supported on reduced graphene oxide and pcdtbt. Adv Funct Mater, 2014, 24: 1904-1910
23 Heo H, Lee MH, Yang J, et al. Assemblies of colloidal CdSe tetrapod nanocrystals with lengthy arms for flexible thin-film transistors. Nano Lett, 2017, 17: 2433-2439
24 Choi CL, Koski KJ, Sivasankar S, et al. Strain-dependent photoluminescence behavior of CdSe/CdS nanocrystals with spherical, linear, and branched topologies. Nano Lett, 2009, 9: 3544-3549
25 Cheng J, Hao J, Liu H, et al. Optically active CdSe-dot/CdS-rod nanocrystals with induced chirality and circularly polarized luminescence. ACS Nano, 2018, 12: 5341-5350
26 Lim J, Bae WK, Park KU, et al. Controlled synthesis of CdSe tetrapods with high morphological uniformity by the persistent kinetic growth and the halide-mediated phase transformation. Chem Mater, 2013, 25: 1443-1449
27 Peng X, Manna L, Yang W, et al. Shape control of CdSe nanocrystals. Nature, 2000, 404: 59-61
28 Peng ZA, Peng X. Nearly monodisperse and shape-controlled CdSe nanocrystals via alternative routes: Nucleation and growth. J Am Chem Soc, 2002, 124: 3343-3353
29 Liu R, Hao J, Li J, et al. Causal inference machine learning leads original experimental discovery in CdSe/CdS core/shell nanoparticles. J Phys Chem Lett, 2020, 11: 7232-7238
30 Hao J, Li Y, Miao J, et al. Ligand-induced chirality in asymmetric CdSe/CdS nanostructures: A close look at chiral tadpoles. ACS Nano, 2020, 14: 10346-10358
31 Gao D, Zhang P, Sheng Z, et al. Highly bright and compact alloyed quantum rods with Near Infrared Emitting: A potential multifunctional nanoplatform for multimodal imaging in vivo. Adv Funct Mater, 2014, 24: 3897-3905
32 Yu WW, Wang YA, Peng X. Formation and stability of size-, shape-, and structure-controlled CdTe nanocrystals: Ligand effects on monomers and nanocrystals. Chem Mater, 2003, 15: 4300-4308
33 Mohamed MB, Tonti D, Al-Salman A, et al. Synthesis of high quality zinc blende CdSe nanocrystals. J Phys Chem B, 2005, 109: 10533-10537
34 Zhou Z, Wang K, Zhang Z, et al. Highly polarized fluorescent film based on aligned quantum rods by contact ink-jet printing method. IEEE Photonics J, 2019, 11: 1-11
35 Gao Y, Peng X. Crystal structure control of CdSe nanocrystals in growth and nucleation: Dominating effects of surface *versus* interior structure. J Am Chem Soc, 2014, 136: 6724-6732
36 Nan W, Niu Y, Qin H, et al. Crystal structure control of zinc-blende CdSe/CdS core/shell nanocrystals: Synthesis and structure-dependent optical properties. J Am Chem Soc, 2012, 134: 19685-19693
37 Peng X. Mechanisms for the shape-control and shape-evolution of colloidal semiconductor nanocrystals. Adv Mater, 2003, 15: 459-463
38 Qu L, Peng ZA, Peng X. Alternative routes toward high quality CdSe nanocrystals. Nano Lett, 2001, 1: 333-337

39 Cao G, Lynch VM, Yacullo LN. Synthesis, structural characterization, and intercalation chemistry of two layered cadmium organophosphonates. Chem Mater, 1993, 5: 1000-1006
40 Fredoueil F, Evain M, Massiot D, et al. Synthesis and characterization of two new cadmium phosphonocarboxylates $Cd_2(OH)(O_3PC_2H_4CO_2)$ and $Cd_3(O_3PC_2H_4CO_2)_2\cdot 2H_2O$. J Chem Soc, Dalton Trans, 2002, 1508-1512

Acknowledgements. MHD acknowledges the CNRS through the MITI interdisciplinary programs (Action MITI: Nouveaux Matériaux 2020 and 2021). This work was financially supported by the Ministry of Science and Technology of China (Nos. 2021YFB3602703 and 2022YFB3602903), National Natural Science Foundation of China (Nos. 62204107, 12204229), Natural Science Foundation of Guangdong Province (No. 2022A1515011614), Shenzhen Key Laboratory for Advanced Quantum Dot Displays and Lighting (No. ZDSYS201707281632549). TEM and HR-TEM observations were performed on microscopes either at Plateforme Aquitaine de Caractérisation des Matériaux (PLACAMAT, UMS 3626, CNRS, Univ. de Bordeaux, Pessac, France) or at Southern University of Science and Technology Core Research Facilities. The authors acknowledge Marion Gayot for the discussions and help at PLACAMAT and the technical support from Dongsheng He and Yang Qiu in SUSTech CRF.

Author contributions Sun X. W. and Delville M-H designed the study; Hao J., Liu H., and Zhou Z. performed the synthesis experiments; Duan X., Zhao B., and Zhang W. carried out most measurements and characterizations; Hao J., Xu B., and Delville M-H wrote the paper. All authors contributed to the general discussion.

Conflict of interest: The authors declare that they have no conflict of interest.

Supplementary information Experimental details and supporting data (UV-vis. spectra and physical characterizations of the various obtained morphologies under the different conditions measured by TEM on at least 200 nanoobjects) are available in the online version of the paper.

Junjie Hao is currently an Associate Professor in the College of Integrated Circuits and Optoelectronic Chips, at Shenzhen Technology University. He received his Ph.D. degree from the University of Bordeaux in 2021. His current research focuses on semiconductor nanocrystal materials and their applications in optoelectronic devices.

Haochen Liu received a bachelor's degree from Wuyi University in 2016. After that, He worked on research at Southern University of Science and Technology (SUSTech) for five years. In 2022, he earned a master's degree from City University of Hong Kong (CityU). He is currently pursuing his Ph.D. degree at CityU, and his primary research interests involve the exploration of perovskite nanocrystals and their potential applications in optoelectronic devices.

Xiao Wei Sun is currently a Chair Professor at the Southern University of Science and Technology, Shenzhen, China. Before joining the Southern University of Science and Technology, he worked at Nanyang Technological University, Singapore, as a Full Professor. He was the Director of the Microelectronics Center at Nanyang Technological University. His main research is currently on semiconductor nanocrystals for power-saving high-quality displays and lighting.

Marie-Helene Delville is currently a Senior Scientist (DR1) at ICMCB CNRS, Univ. Bordeaux, FRANCE. She received a Ph.D. degree at the University of Bordeaux. Her research interests are focused on the fundamental and practical aspects of the synthesis of organic-inorganic colloidal nano-objects with special emphasis on synthesis, shape control, surface functionalization of inorganic nanoparticles & sol-gel chemistry.

CdSe/CdS纳米晶在壳层形成和生长过程中的形貌调控：表面配体对晶体结构的决定性作用

郝俊杰[1,2,3#*]，刘皓宸[2,4#]，段西健[2,5]，周子明[2,5]，赵冰心[2]，张文达[2,7]，徐冰[6]，孙小卫[2,5,6*]，Marie-Helene Delville[1*]

摘要 CdSe/CdS纳米晶是研究最多的纳米晶之一，然而，仍有许多领域有待研究. 这项工作揭示了核-壳纳米晶的形貌控制主要由表面配体、核心浓度控制，而非核心的晶体结构. 其中，羧酸镉促进各向同性结构的生长，而相反的，长链膦酸镉有利于各向异性结构的制备. 对于蝌蚪形貌纳米晶，羧酸镉对于头部壳层影响较大，而膦酸镉在各向异性尾部生长中起主要作用. 与预期相反，CdSe核心的晶体结构（闪锌矿或纤锌矿）在决定最终的晶体形貌方面几乎没有作用，这可能是由于CdS壳层两个阶段的生长，并导致了蝌蚪形貌的生成. 通过选择恰当的表面配体，可以在CdSe/CdS核壳结构形成和生长过程中精确的调控其形貌. 在我们的工作中，蝌蚪、纳米花、点-棒结构、多足结构均可以通过调控表面配体的比率而获得. 这种独特的晶体生长机制可以应用于其他基于种子生长的工艺以构筑各向异性纳米结构.

Table of contents (TOC)

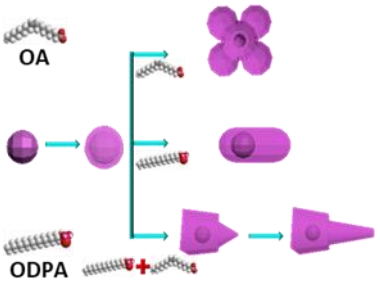

By adjusting the ratio between two functional ligands usually used separately in the synthesis of CdSe/CdS NCs, (OA and ODPA), one-pot synthesis of nanostructures is performed leading to different controlled morphologies such as Tadpoles, Nanoflowers, DRs, and Tetrapods